

# Stochastic Process of Multiple Cracking in Discontinuous Random Fiber Reinforced Brittle Matrix Composites

HWAI-CHUNG WU AND VICTOR C. LI\*

*Advanced Civil Engineering Materials Research Laboratory  
Department of Civil and Environmental Engineering  
University of Michigan  
Ann Arbor, MI 48109, USA*

**ABSTRACT:** The classical ACK model for multiple cracking in a tensile specimen of a fiber reinforced brittle matrix composite does not account for flaw size distribution of the matrix. In this paper, a stochastic treatment of the damage process in the form of multiple cracking in discontinuous random fiber reinforced brittle matrix composites is presented. The effect of matrix flaw size distribution (initial matrix damage) on composite strength and crack spacing is analyzed. The flaw size distribution of the matrix is simulated by a Monte Carlo process. In the simulation, a Weibull-type function is assumed. The conditions for crack growth depending on initial flaw size and external loads as well as fiber bridging effect are highlighted. Unique merits and deficiencies of the current study are also discussed.

**KEY WORDS:** fiber composite, multiple cracking, fracture mechanics, stochastic simulation.

## 1. INTRODUCTION

**I**N BRITTLE MATERIALS such as concrete and ceramics, fiber reinforcement is commonly used to improve their strength and toughness (Evans, 1990; Shah, 1991a; Shah, 1991b). Further benefits by addition of fibers include pseudo strain-hardening behavior and notch insensitivity. The former leads to much enhanced ductility (Marshall and Cox, 1987; Wu and Li, 1994), whereas the latter contributes to improved composite reliability (Leung and Li, 1989; Marshall et al., 1985).

In pseudo strain-hardening composites, extensive damage can be observed on

---

\*Author to whom correspondence should be addressed.

the specimen after first crack load in a uniaxial tension test (Li and Wu, 1992). Sub-parallel cracks are formed on the matrix as the load increases towards the composite ultimate strength, which can be several times higher than the first crack strength. The multiple cracks, bridged by fibers, contribute to the continued inelastic tensile strain, and are typically accompanied by a significantly reduced stiffness in comparison to the undamaged material. This damage process is terminated when one of the multiple cracks opens up as the bridging load acting across this crack softens, when fibers are pulled-out and thus localizing the failure onto this crack plane.

Continuum damage mechanics (CDM) considers a uniform damage over the volume of materials prior to damage localization, and shows how the load carrying capability of given cross-sections is deteriorated by a single quantity  $\omega$  (damage parameter) (Kachanov, 1958, 1961; Fanella and Krajcinovic, 1985; Krajcinovic, 1979; Loland, 1980). In the past, CDM has been applied to study the mechanical properties of brittle materials as well as fiber reinforced brittle matrix composites (Fanella and Krajcinovic, 1985; Krajcinovic and Fonseka, 1981; Loland, 1980). While often complicated, there is an increasing trend in CDM research towards more physically based modelling (Ju and Lee, 1991; Lee and Ju, 1991; Sumarac and Krajcinovic, 1989), in which physical parameters can be experimentally measured.

In this paper, attention is given to the evolution of matrix cracking originated from preexisting defects. Initial damage including pores and cracks in the composites will become activated to grow at various external loads. It should be noted that initial damage depends on existing flaws due to processing as well as cracks generated by shrinkage or other environmental effects at the time of testing.

Aveston et al. (1971) first proposed the conditions for multiple cracking in continuous aligned fiber reinforced brittle matrix composites, notably known as the ACK theory, and lay the foundation for subsequent research (Li and Leung, 1992; Li and Wu, 1992; Marshall et al., 1985). In these models, uniform distribution of identical flaw size in the matrix is implicitly assumed. Consequently, a deterministic composite strength during multiple cracking is predicted, and usually does not agree well with experimental findings, as shown in Figure 1 for a discontinuous random polyethylene fiber reinforced cement. This discrepancy is also found in a continuous aligned SiC reinforced calcium aluminosilicate (Cho et al., 1992; Yang and Knowles, 1993). A rising load carrying capacity beyond the first cracking strength during multiple cracking resembles strain hardening of metals, often referred to as pseudo strain-hardening. Multiple cracks develop over a wide range of load levels. Besides the difference in observed stress-strain curves, the distribution of crack spacing also shows evidence against the assumption of identical flaw size. A simple calculation can be used to compute the crack spacing,  $x$ , on the basis of force balance (Aveston et al., 1971; Wu and Li, 1992).

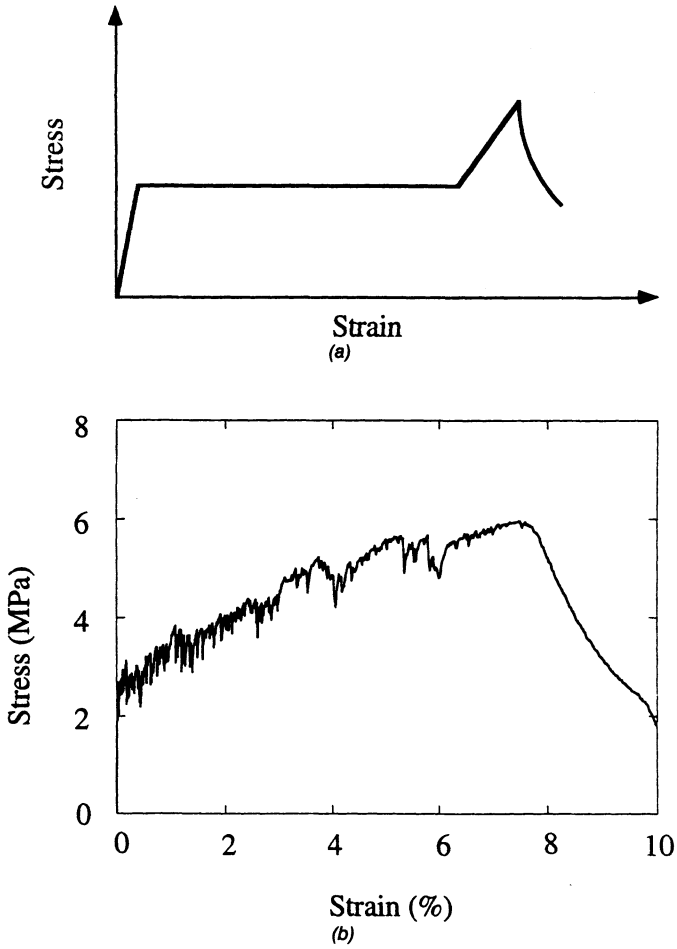


**Figure 1.** (a) Schematic representation of tensile stress-strain curve of fiber composites with a deterministic matrix strength (b) experimental stress-strain curve of random discontinuous polyethylene fiber reinforced cement paste ( $V_f = 2\%$ ,  $L_f = 12$  mm, plasma treated).

$$x = \frac{V_m \sigma_{mu} R}{2V_f \tau} \quad \text{for continuous aligned fiber} \quad (1)$$

where  $V_m$  and  $V_f$  are the volume fractions of the matrix and the fiber,  $R$  is the radius of the fiber,  $\sigma_{mu}$  is the single-valued matrix cracking stress, and  $\tau$  is a constant shear stress.

and

$$x_a = \frac{L_f - \sqrt{L_f^2 - 2\pi L_f \psi x}}{2} \quad \text{for discontinuous random fiber} \quad (2)$$

where  $L_f$  is the fiber length,  $\psi$  ( $= 4/\pi g$ ) is the correction factor for 3-D fiber randomness,  $g$  is the snubbing factor, and  $x$  is defined in Equation (1). Hence after crack saturation, a final crack spacing of between  $x$  and  $2x$  is expected. Kimber and Keer (1982) have calculated the average value of the crack spacing for multiple matrix cracking when the matrix strength is a deterministic value, based on analogy with minimum average spacing between cars of length  $x$  parked at random in an infinite line. Their results yield an average spacing of  $1.337x$ . However, experimental observations of multiple crack spacing in steel/epoxy (Cooper and Sillwood, 1972), in carbon/glass (Yang and Knowles, 1992), and in SiC/calcium aluminosilicate (Cho et al., 1992) do not support this prediction. Instead, better agreements between theory and experiment are found when a distribution of matrix cracking strength is assumed (Cho et al., 1992; Cooper and Sillwood, 1972; Yang and Knowles, 1992).

Regarding the nature of the distribution of matrix cracking strength in composites, it is not yet well understood. The origin of such strength distribution may be attributable to 1) a distribution of matrix flaw sizes, 2) interaction of matrix cracks, and 3) variation of fiber reinforcement. The first two factors have been recently examined by Zok and Spearing (Spearing and Zok, 1992; Zok and Spearing, 1992) for a unidirectional SiC/CAS composite. The variation of fiber reinforcement includes interfacial bond strength ( $\tau$ ) and volume fraction ( $V_f$ ) within the composites. These non-uniformity are generally caused by the processing of the composites. Even in the continuous aligned fiber composites, fiber volume fraction still varies (Barron-Antolin et al., 1988; Prewo and Brennan, 1982). Non-uniform fiber dispersion in a discontinuous random fiber composite is more profound when severe fiber entanglement or poor workability occurs. In addition, Kagawa and Honda (1991) discovered a distribution of frictional bond strength of unidirectional SiC/LAS by protrusion method. The implications of such variations in  $\tau$  and  $V_f$  is that the composite property may vary from location to location via the bridging law (bridging stress versus crack opening relationship),  $\sigma(\delta)$ , which is locally dependent.

For unidirectional composites to which most ceramic based composites belong, in addition to the distribution of the matrix cracking strength, the strength of the fiber also follows a distribution which governs the magnitude of the achievable toughness due to fiber pullout after fiber fracture inside the matrix (Curtin, 1991; Knowles and Yang, 1992; Sutcu, 1989). Research on discontinuous random fiber composites is much scant. Nevertheless, rapidly growing demands for fundamental understanding of the mechanical behavior of discontinuous random fiber composites call for closer examination of the pseudo strain-hardening phenomenon in such composites which might possess processing ease and low cost compared to continuous aligned system. This is particularly important in cost-sensitive applications such as in the construction industry.

In this paper, focus is placed on modelling the damage evolution during strain-hardening in discontinuous random fiber reinforced brittle matrix composites. A stochastic treatment of multiple cracking is presented based on the weakest link concept originally proposed by Weibull (1951). The flaw size distribution of the matrix is simulated by a Monte Carlo process. Consequently, the effect of matrix flaw size distribution (initial matrix damage) on composite strength and crack spacing is analyzed and discussed. The issue of variable bond strength ( $\tau$ ), fiber volume fraction ( $V_f$ ), and fiber strength ( $\sigma_{fu}$ ) is not addressed in the present work.

## 2. RELEVANT MECHANICS

The current analysis for matrix crack propagation is based on fracture mechanics approach where matrix damage is related to the most critical flaw (e.g., dominant crack oriented perpendicular to the loading direction) at a given cross-section of the composite. The matrix of the section of the composite is considered totally damaged when a crack runs through the entire cross-section resulting in complete loss of load-carrying capability. Nevertheless, the composite can still survive if the bridging fibers can bear the additional loads. "Fiber damage" is related to debonding process followed by either fiber pull-out or rupture. Matrix damage can be progressively developed throughout the composite and finally completed at all sections without the formation of localized fracture zone of the composite, whereas fiber damage can occur independently of matrix damage and throughout the composite until a complete failure is reached at a particular section. The uniqueness of fiber reinforced brittle matrix composites exhibiting pseudo strain-hardening behavior includes the co-existence of the process of matrix and fiber damage as well as uniform complete damage in the matrix prior to composite failure.

The conditions for pseudo-strain-hardening in discontinuous random fiber reinforced brittle matrix composites have been formulated and discussed in detail elsewhere (Li and Leung, 1992; Li and Wu, 1992; Li et al., 1994). Only a brief description is given as follows. The pseudo strain-hardening process is made possible by the stress transfer capability of *adequately* designed fiber reinforce-

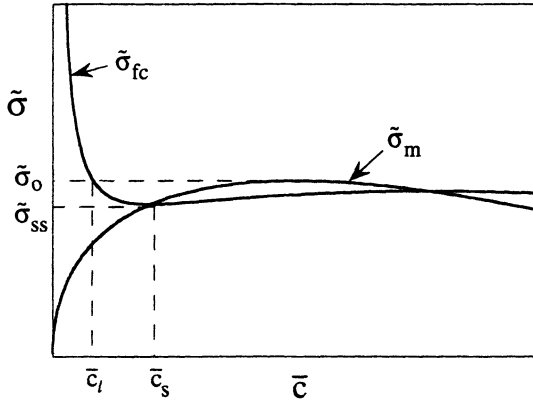


**Figure 2.** First crack strength and bridging stress at midcrack position; conditions for steady state cracking requires these curves to meet, i.e.,  $\bar{K} < \bar{K}_{crit}$  (normalization is made by  $\tilde{\sigma} = \sigma/\sigma_0$ ,  $\sigma_0 = \sqrt{1}\tau(L_f/d_f)/2$  and  $\bar{c} \equiv \sqrt{c/c_0}/\delta^*$  where  $c =$  flaw size,  $c_0 = [L_f E_c/2K_{tip} [\pi/16(1 - \nu^2)^2]$ ,  $\delta^* = (2\tau/(1 + \eta)E_f)(L_f/d_f)$ , and  $\eta = (\sqrt{1}E_f)/(\sqrt{V_m}E_m)$ ).

ment in the composite. The role of fibers is primarily twofold. First, the bridging action of fibers should provide sufficient toughness relative to crack tip toughness so that the critical crack can propagate in a “steady-state” manner. In fiber composites, the extension of a matrix crack is accompanied by fiber bridging across the crack flanks. The bridging stress increases as the crack opens until reaching the same magnitude of the applied loads. Subsequently, the crack flanks flatten to maintain the constant applied stress level, and the cracks propagate without any further increase in applied loads. Figure 2 illustrates such requirements for steady-state cracking schematically. Second, the maximum bridging stress ( $\sigma_0$ ) imposed by fiber/matrix interactions should exceed the steady state strength ( $\sigma_{ss}$ ).

$$\sigma_{ss} \leq \sigma_0 \quad (3)$$

Equation (3) provides a general condition for pseudo strain-hardening. This expression includes all relevant microparameters such as fiber property, fiber geometry, matrix property, and interface property. Exact formulation depends on the bridging law specific for a given composite system. For example, in discontinuous random fiber composites in which fiber pull-out is expected (as the case in this study), the bridging law can be derived as (Li, 1992)

$$\sigma(\delta) = \begin{cases} \sigma_0[2(\delta/\delta_0)^{1/2} - (\delta/\delta_0)] & \text{for } \delta \leq \delta_0 \\ \sigma_0(1 - 2\delta/L_f)^2 & \text{for } \delta_0 \leq \delta \leq L_f/2 \\ 0 & \text{for } L_f/2 \leq \delta \end{cases} \quad (4)$$

where  $\delta_0 = \tau L_f^2/[E_f d_f(1 + \eta)]$  is the crack opening corresponding to the maximum bridging stress

$$\sigma_o = g\tau V_f L_f / (2d_f) \tag{5}$$

In Equations (4) and (5),  $V_f$ ,  $L_f$ ,  $d_f$ , and  $E_f$  are the fiber volume fraction, length, diameter and Young's Modulus, respectively.  $\tau$  is the fiber/matrix frictional bond strength, and  $g = 2(1 + e^{f\pi/2}) / (4 + f^2)$  where  $f$  is a snubbing coefficient (Li et al., 1990) which must be determined experimentally for a given fiber/matrix system. The snubbing coefficient raises the bridging stress of fibers bridging at an angle inclined to the matrix crack plane, appropriate for flexible fibers exiting the matrix analogous to a rope passing over a friction pulley. Finally,  $\eta = (V_f E_f) / (V_m E_m)$ , where  $V_m$  and  $E_m$  are the matrix volume fraction and Young's Modulus, respectively.

The above conditions can be graphically shown in Figure 3 where normalized first crack strength is expressed as a function of  $\bar{K}$  and  $\bar{c}$ ;  $\bar{K}$  is the ratio of crack tip fracture energy absorption rate to the energy absorption rate in the fiber bridging zone behind the crack front whereas  $\bar{c}$  is the normalized flaw size. For a composite with a  $\bar{K}$  larger than  $\bar{K}_{crit}$ , the material will fail immediately at the first crack strength. Although toughened by the presence of fibers, the composite remains essentially notch-sensitive as in a Griffith material. For a composite with a  $\bar{K}$  smaller than  $\bar{K}_{crit}$ , the material will undergo multiple cracking at the steady-state strength ( $\sigma_{ss}$ ), and fail at the maximum bridging stress ( $\sigma_o$ ). The material strength becomes independent of flaw size, as long as  $\bar{c}$  is larger than  $\bar{c}_s$ , where  $\bar{c}_s$  is defined by the value of  $\bar{K}$  (details refer to Li and Leung, 1992). In addition, there is a range of  $\bar{c}_i < \bar{c} < \bar{c}_s$  (Figure 2), for which multiple cracking is guaranteed.

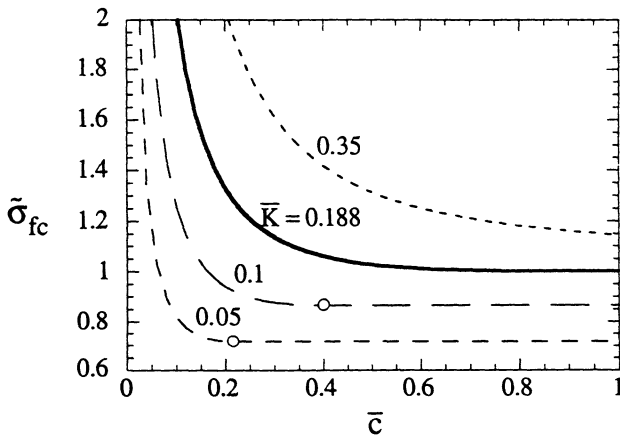


Figure 3. First crack strength decay with flaw size; for  $\bar{K} > \bar{K}_{crit} = 0.188$ , material remains notch-sensitive; for  $\bar{K} < \bar{K}_{crit} = 0.188$ , material becomes notch-insensitive in plateau region (circle indicates the beginning of the plateau, i.e.,  $\bar{c}_s$ ).

### 3. COMPUTER SIMULATION

The position and size distribution of matrix flaws are, in general, random occurrences. Thus, the event of the failure can be modeled as a stochastic process and will be approached here based on statistical analysis. To simulate the formation of multiple matrix cracks from various flaw size under tension, a one-dimensional array of volume elements, each of unit cross-sectional area, is used. A flaw size is then assigned to each element by Monte-Carlo simulation. It refers to the use of mathematical models to study systems that are characterized by the occurrence of discrete, random events (Gottfried, 1984). These individual events are represented by random variables whose values are generated by a computer, and governed by a Weibull distribution function as below:

$$F(c,L) = \exp \left[ - \frac{L}{L_o} \left( \frac{c_o}{c} \right)^m \right] \quad (6)$$

where  $F$  is the cumulative probability of flaws having size smaller than  $c$  in an element of length  $L$ ,  $m$  is the shape parameter (or Weibull modulus) and  $c_o$  and  $L_o$  are the reference flaw size and element length. The above notation follows Spearing and Zok (1992), which gives better physical meaning to  $c_o$  taken to be  $c_s$  (Figure 2). For convenience, let  $L_o = \lambda x_d$  where  $x_d$  is the crack spacing of a discontinuous random fiber system [Equation (2)], and  $\lambda$  is the dimensionless scaling factor and a measure of the population of flaw size in relation to the reference flaw size  $c_o$ . For large  $\lambda$ , a significant number of initial flaws have a size less than  $c_o$ . The element length  $L$  is typically a fraction of  $x_d$  and 1/10 is used in the current calculation with a long gage length of  $100 x_d$ . Hence a total volume element of 1000 is used in the simulation process. The flaw size distributions are shown in Figure 4 for  $m = 2$  and 10.

It should be noted that Equation (6) is formulated on the basis of flaw size distribution which will then be used to compute the strength of the composites through the relationships described in the mechanics section. This is different from the strength distribution approach (Cho et al., 1992; Mihashi, 1983) where a probability function is expressed in term of strength directly. A factor of two difference appears in the shape parameter ( $m$ ) of linear-elastic-fracture-mechanics materials for these two formulations.

The simulation of matrix cracking proceeds as follows. Once a flaw size,  $c$ , is assigned to a given element,  $c$  will be checked against the crack growth criteria (Figure 2):

1.  $c > c_s$ . This is the case of steady state cracking. Hence the composite strength (= first cracking strength) is equal to the steady state strength, i.e.,  $\sigma_c = \sigma_{fc} = \sigma_{ss}$ .
2.  $c_s > c > c_i$ . Multiple cracking can still occur with increasing composite strength until reaching the maximum bridging strength, i.e.,  $\sigma_c > \sigma_{ss}$ .



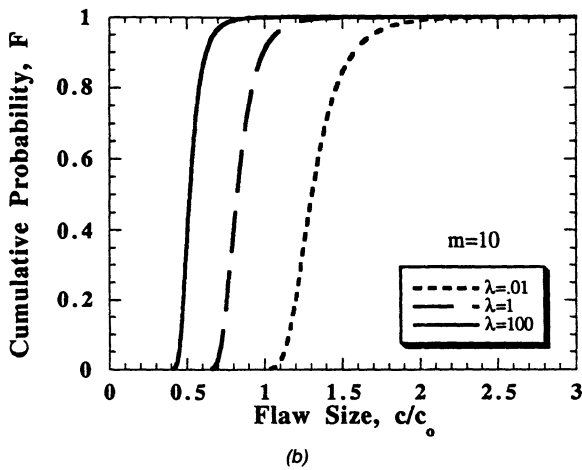
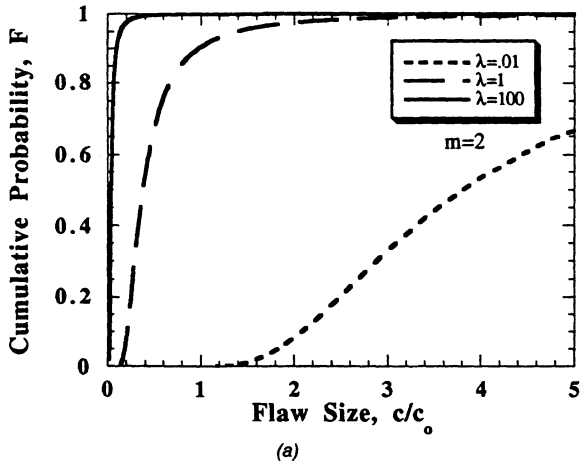


Figure 4. Flaw size distributions (a)  $m = 2$  (b)  $m = 10$ .

3.  $c < c_l$ . No further crack propagation is possible, since the composite strength is limited by the maximum bridging strength ( $\sigma_o$ ), i.e.,  $\sigma_c \leq \sigma_o$ . This marks the end of multiple cracking.

After all flaws have been examined at a given stress level, the stress is incremented and the process is repeated until the maximum bridging strength is reached. At each stage, the distribution of crack spacing is determined.

#### 4. EVOLUTION OF MATRIX CRACKING

Typical results of the simulations on crack spacing distribution are presented in Figure 5 at two levels of stress for  $m = 2$  and  $\lambda = 300$ . Similar trends are obtained for other pairs of  $m$  and  $\lambda$ . Since there is no available data on  $m$  and  $\lambda$  for the matrix used in our experiments,  $m = 2$  is chosen based on reported values ranging from 4 to 8 (after conversion from strength based function to flaw size based function) for plain cement and concrete in the literature (Ashby and Jones, 1986; Mihashi, 1983). A slightly lower value was used in order to account for the additional flaws induced by the reinforcing fibers (2% fiber reinforcement used in the experiment). In the current study,  $\lambda$  is treated as an adjusting parameter to fit the experimentally determined cracking frequency versus composite strength curve. As shown in Figure 6, a good match is found when  $\lambda$  is equal to 300. Hence  $m = 2$  and  $\lambda = 300$  are used throughout in this study.

Materials used in this study consist of type I Portland cement, silica fume and superplasticizer with water/cementitious ratio of 0.27. Discontinuous polyethylene fibers ( $L_f = 12$  mm,  $d_f = 38$   $\mu$ m, and  $E_f = 120$  GPa) were used as-received to reinforce the paste at a volume fraction of 2%. Tensile coupon specimens of size  $304.8 \times 76.2 \times 12.7$  mm were prepared and tested under direct tension in a servo hydraulic tester. Detailed mix proportions and testing procedure can be found elsewhere (Li et al., 1994).

##### 4.1 Distribution of Composite Strength

It was observed during the experiments that the locations of matrix cracking occurred randomly within the available gage length, beginning at  $\sigma_{cr}$  and ending at  $\sigma_o$ . A video camera is set up next to the specimens and continuously record the occurrence of cracking. Crack spacing distribution can then be analyzed on computer with the aid of frame grabber and image analysis program at any given load levels. The stress-strain curve plotted together with the average crack spacing vs strain of the polyethylene fiber reinforced cement paste clearly show the coincidence of crack saturation with the peak load (i.e.,  $\sigma_o$ ) in Figure 7. In this case, the composite strength during multiple cracking varies from 2 MPa to 3.3 MPa. A picture showing crack evolution with composite strain level is presented in Figure 8.

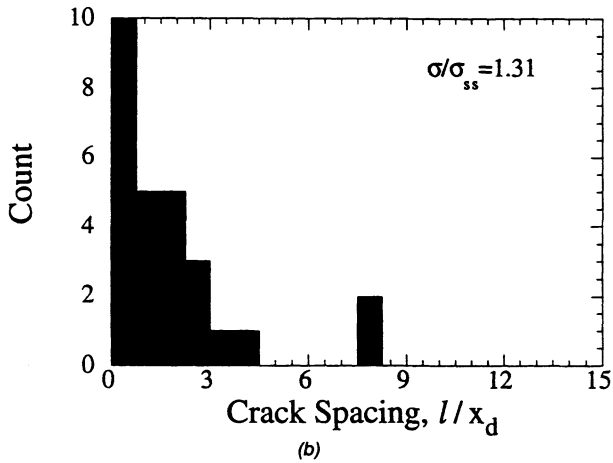
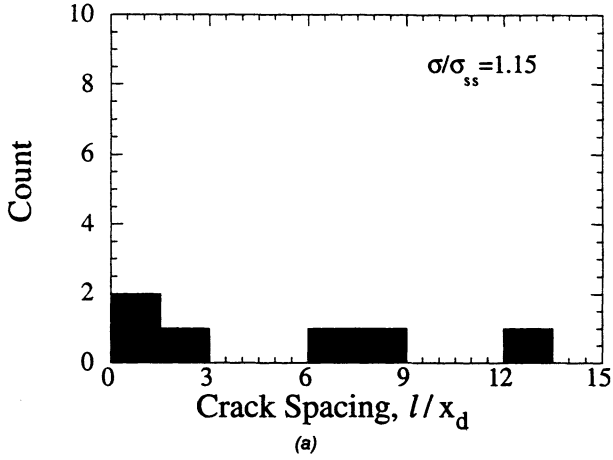
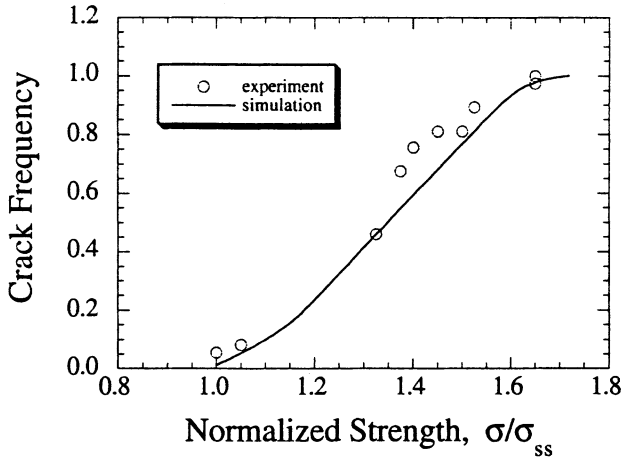
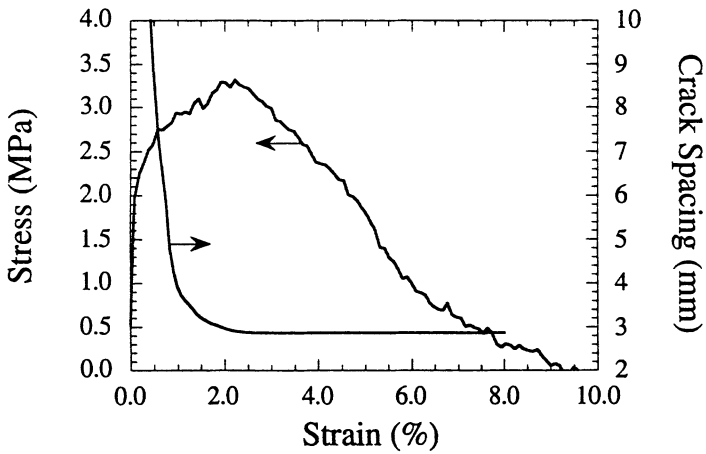


Figure 5. Histograms of crack spacing at two levels of applied stress ( $m = 2$  and  $\lambda = 300$ ) (a)  $\sigma/\sigma_{ss} = 1.15$  (b)  $\sigma/\sigma_{ss} = 1.31$ .



**Figure 6.** Comparison of crack frequency vs composite strength (normalized by the steady state strength  $\sigma_{ss}$ ) between experimental data and simulation results,  $m = 2$  and  $\lambda = 300$ .



**Figure 7.** Tensile stress-strain curve of a discontinuous random polyethylene fiber reinforced cement paste ( $V_f = 2\%$ ), together with corresponding average crack spacing.

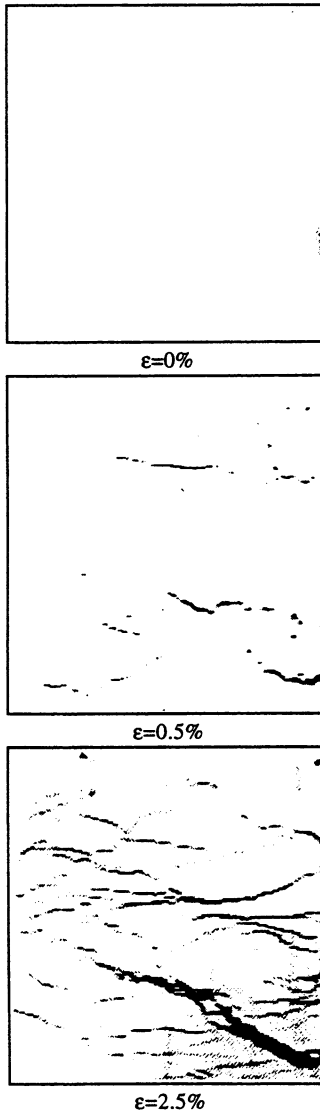


**Figure 8.** Computer scanned image of crack evolution at various load levels (see Figure 7) during multiple cracking (frames showing approximately same locations).

## 4.2 Distribution of Crack Spacing

Crack spacing (normalized by  $x_d$ ) can be plotted against composite strength (normalized by  $\sigma_{sa}$ ), as shown in Figure 9 where  $x_d$  is computed to be 2.2 mm [from Equation (2)]. In deriving  $x_d$ ,  $\sigma_{mu}$  (= 2 MPa) is taken from the experimental data,  $\tau$  (= 0.66 MPa) is deduced from the maximum bridging stress, and the snubbing factor  $g$  is assumed to be 1.5 (Li and Wu, 1992). A good agreement of average crack spacing vs composite strength is obtained between the simulation and experimental results. This comparison is made on the basis of average crack spacing. However, experimentally determined distribution of crack spacing after crack saturation differs with the simulation. As revealed in Figure 10, the simulation gives a higher portion of small and large crack space compared to the experimental data, although both of them have same average value. This discrepancy is probably caused by crack interaction which is not considered in the present simulations. Zok and Spearing (1992) suggested that interactions between adjacent cracks lead to reduced strain energy release rate when the crack spacing falls below twice the slip length [i.e.,  $x$  in Equation (1)] for continuous aligned fiber composites. Hence cracking is prohibited within immediate neighborhood of existing cracks until external loads are further increased.

## 5. OBSERVATION OF CRACK WIDTH DISTRIBUTION

In addition to distributions of composite strength and crack spacing due to distribution of matrix flaw, it is observed that crack width also follows a distribution

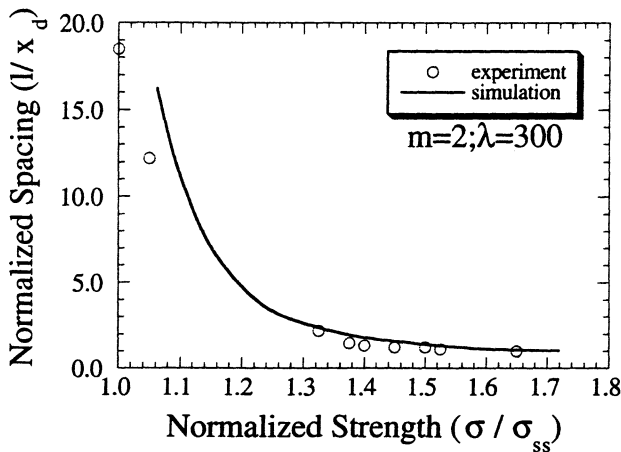
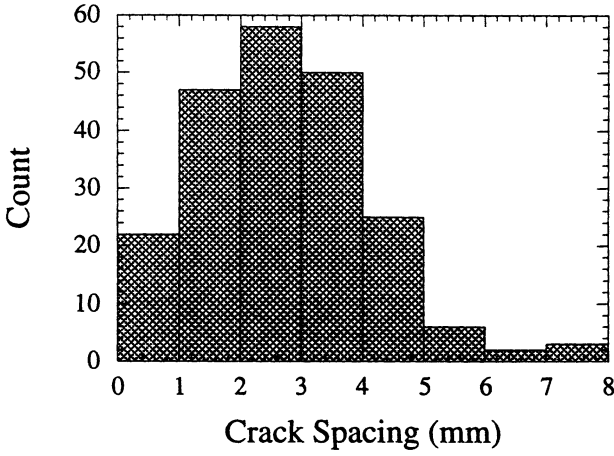
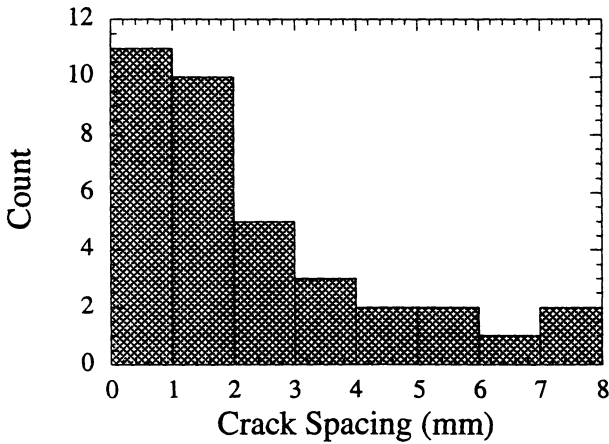


**Figure 9.** Comparison of average crack spacing (normalized by  $x_d$ ) vs composite strength (normalized by  $\sigma_{sa}$ ) after first cracking of a polyethylene fiber reinforced cement paste ( $V_f = 2\%$ ) between experimental data and simulation results.



(a)



(b)

**Figure 10.** Distributions of crack spacing (a) experimental data (b) simulation results. The total counts of the experimental data are obtained by measuring crack spacing along three parallel lines drawn on the specimen.

instead of a single value. This is shown in Figure 11 for the same polyethylene fiber cement. The crack width ranges from 20  $\mu\text{m}$  up to 800  $\mu\text{m}$ . This variation suggests that the common assumption of single bridging law ( $\sigma$ - $\delta$  curve, details refer to Li, 1992) which governs the mechanical behavior of the composite is questionable. Otherwise, force equilibrium should ensure identical crack opening (or crack width) along the specimen length. At present, there is limited evidence showing variation of bond strength ( $\tau$ ) and fiber distribution (particularly

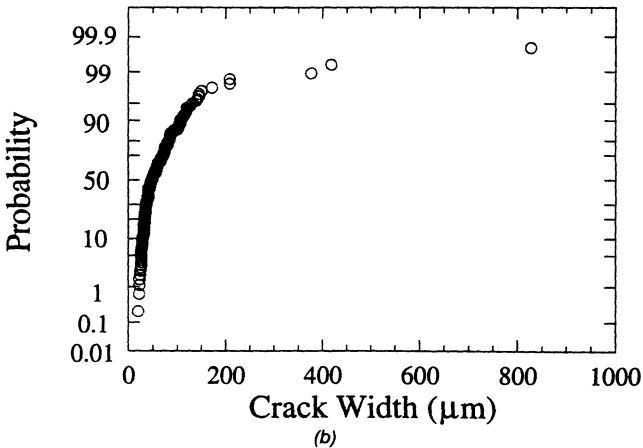
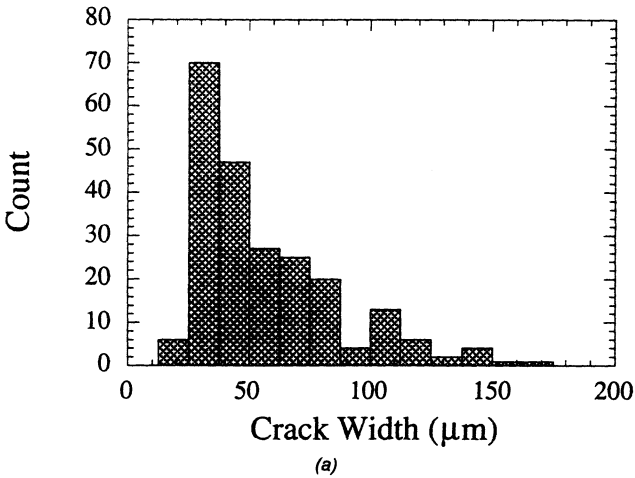


**Figure 11.** Distribution of crack width of polyethylene fiber cement (a) frequency (b) cumulative probability.



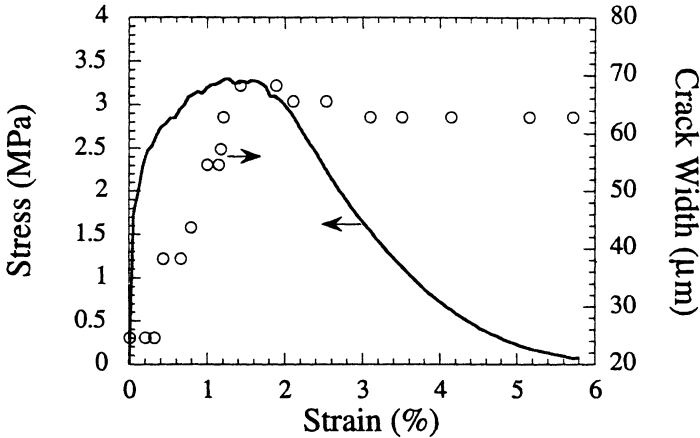


**Figure 12.** Plot of crack width vs stress and strain showing insignificant crack closure after completely unloading, polyethylene fiber reinforced cement ( $V_f = 2\%$ ).

fiber volume fraction,  $V_f$ ) in the composite, which may be responsible for the variation in  $\sigma$ - $\delta$  relationship. Therefore, the matrix strength distribution during multiple cracking may result from distribution of matrix flaw, crack interaction, and variation in  $\sigma$ - $\delta$  relation. This issue deserves further study.

The crack width measurement was conducted using a microscope with 50 times magnification on the specimens surfaces after complete unloading. Complete crack closure cannot occur upon unloading due to a reversed frictional stress which prevents fibers from slipping back into the matrix when the specimens are unloaded (Wu et al., 1994). This is demonstrated in Figure 12. The reduction in crack width is typically less than 10% after complete unloading from peak load. Hence no attempt has been made to correct the effect of crack closure on crack width measured after the specimens are completely unloaded.

## 6. FURTHER DISCUSSION

The current study presents an initial attempt at combining the mechanics aspects of fiber bridging in composites with the stochastic aspects of matrix flaw size and location for discontinuous random fiber composites. The details of the mechanics of extension of a bridged crack and the effect of fiber bridging on composite properties, especially the pseudo strain-hardening behavior, are described by the more fundamental bridging law, i.e.,  $\sigma$ - $\delta$  relationship, which involves all relevant microparameters [Equation (4)].

In addition, the matrix fracture toughness ( $K_m$ ) also contribute to composite strength (first cracking strength and/or steady state strength) which is determined from a balance of stress intensity factors associated with the applied load, that

with fiber bridging effect and the crack tip fracture toughness (Li and Leung, 1992; Marshall et al., 1985). In the current calculation (see Figures 2 and 3), an elliptical crack profile is assumed for mathematical tractability. Further, a unique  $\sigma$ - $\delta$  relationship and  $K_m$  are specified throughout the composite. In reality, the crack profile is expected to deviate from the elliptical shape since the cohesive tractions acting on the crack flank vary depending on the crack opening via the  $\sigma$ - $\delta$  relationship. The actual crack shape can be obtained by numerical analysis (Danchaivijit and Shetty, 1993; Marshall et al., 1985). This correction is currently being investigated by the authors. Since the non-uniform  $K_m$  and  $\sigma(\delta)$  due to processing is not taken into account yet, the current parametric values obtained for the Weibull function of flaw size distribution should be used with caution. Nevertheless, these corrections (crack shape,  $K_m$  and  $\sigma(\delta)$  non-uniformity) can be readily accommodated in the current mechanics framework. Finally, it should be noted that the preceding scheme is valid when the crack length is large compared to the fiber spacing so that bridging stress can be treated as a continuous pressure acting on the crack face. This also implies that all cracks under consideration are bridged by fibers. The effect of short cracks (unbridged cracks) on composite strength is not included in this study.

## 7. CONCLUSION

Multiple cracking in discontinuous random fiber reinforced brittle matrix composites is studied and simulated by a Monte Carlo process in this paper. A good agreement of composite strength and average crack spacing between experiment data and simulation results is found for a polyethylene fiber reinforced cement paste ( $V_f = 2\%$ ). A somewhat different distribution of crack spacing after crack saturation is predicted from the simulation. This is probably caused by crack interactions which are not considered in the present study.

The current approach combining mechanics aspect of crack propagation and stochastic aspect of flaw distribution provides better understanding and physical explanation of the pseudo strain-hardening behavior of fiber composites. Preliminary data suggest that the condition for crack propagation depend on initial flaw size, external loads, and fiber bridging effect ( $\sigma$ - $\delta$  relation) which may vary in the composites. The last factor has not been recognized previously.

## ACKNOWLEDGMENT

Part of this work has been supported by a grant (BCS-9202097) from the National Science Foundation to the University of Michigan.

## REFERENCES

- Asby, M. F. and D. R. H. Jones. 1986. *Engineering Materials 2*, Pergamon Press.

- Aveston, J., G. A. Cooper and A. Kelly. 1971. "Single and Multiple Fracture," in *The Properties of Fiber Composites*, Guilford, UK: IPC Science and Technology Press, pp. 15–26.
- Barron-Antolin, P., G. H. Schiroky and C. A. Andersson. 1988. "Properties of Fiber Reinforced Alumina Matrix Composites," *Ceram. Eng. Sci. Proc.*, 9(7–8):759–766.
- Cho, C., J. W. Holmes and J. R. Barber. 1992. "Distribution of Matrix Cracks in a Uniaxial Ceramic Composite," *J. Am. Ceram. Soc.*, 75(2):316–324.
- Cooper, G. A. and J. M. Sillwood. 1972. "Multiple Fracture in a Steel Reinforced Epoxy Resin Composite," *J. Mater. Sci.*, 7:325–333.
- Curtin, W. A. 1991. "Theory of Mechanical Properties of Ceramic-Matrix Composites," *J. Am. Ceram. Soc.*, 74(11):2837–2845.
- Danchaivijit, S. and D. K. Shetty. 1993. "Matrix Cracking in Ceramic-Matrix Composites," *J. Am. Ceram. Soc.*, 76(10):2497–2504.
- Evans, A. G. 1990. "Perspective on the Development on High-Toughness Ceramics," *J. Am. Ceram. Soc.*, 73(2):187–206.
- Fanella, D. and D. Krajcinovic. 1985. "Continuum Damage Mechanics of Fiber Reinforced Concrete," *Journal of Engineering Mechanics*, 111(8):995–1009.
- Gottfried, B. S. 1984. *Elements of Stochastic Process Simulation*, Prentice-Hall.
- Ju, J. W. and X. Lee. 1991. "Micromechanical Damage Models for Brittle Solids. I: Tensile Loadings," *J. Engineering Mechanics*, 117(7):1495–1514.
- Kachanov, L. M. 1958. "On the Life-Time under Creep Conditions," *Izvestiya (Bull.) USSR Ac. Sci., Division of Technical Sciences*, 8:26–31 (in Russian).
- Kachanov, L. M. 1961. "Rupture Time under Creep Conditions," in *Problems of Continuum Mechanics*, J. R. M. Radok, ed., Philadelphia: SIAM, 202–218.
- Kagawa, Y. and K. Honda. 1991. "A Protrusion Method for Measuring Fiber/Matrix Sliding Frictional Stresses in Ceramic Matrix Composites," *Ceram. Eng. Sci. Proc.*, 12(7–8):1127–1138.
- Kimber, A. C. and J. G. Keer. 1982. "On the Theoretic Average Crack Spacing in Brittle Matrix Composites Containing Continuous Aligned Fibers," *J. Mater. Sci. Lett.*, 1:353–354.
- Knowles, K. M. and X. F. Yang. 1991. "Mathematical Modeling of the Strength and Toughness of Unidirectional Fiber-Reinforced Ceramics," *Ceram. Eng. Sci. Proc.*, 12(7–8):1375–1388.
- Krajcinovic, D. 1979. "Distributed Damage Theory of Beams in Pure Bending," *Transactions of the ASME*, 46:592–596.
- Krajcinovic, D. and G. U. Fonseka. 1981. "The Continuous Damage Theory of Brittle Materials," *J. Applied Mechanics*, 48:809–815.
- Lee, X. and J. W. Ju. 1991. "Micromechanical Damage Models for Brittle Solids. II: Compressive Loadings," *J. Engineering Mechanics*, 117(7):1515–1536.
- Leung, C. K. Y. and V. C. Li. 1989. "First-Cracking Strength of Short Fiber-Reinforced Ceramics," *Ceram. Eng. Sci. Proc.*, 10(9–10):1164–1178.
- Li, V. C. and C. K. Y. Leung. 1992. "Theory of Steady State and Multiple Cracking of Random Discontinuous Fiber Reinforced Brittle Matrix Composites," *ASCE J. Eng. Mech.*, 118(11):2246–2264.
- Li, V. C. and H. C. Wu. 1992. "Conditions for Pseudo Strain-Hardening in Fiber Reinforced Brittle Matrix Composites," *Appl. Mech. Review*, 45(8):390–398.
- Li, V. C., H. C. Wu, M. M. Maalej, D. K. Mishra and T. Hashida. 1994. "Tensile Behavior of Cement Based Composites with Random Discontinuous Steel Fibers." Submitted for publication in *J. Am. Ceram. Soc.*
- Li, V. C. 1992. "Postcrack Scaling Relations for Fiber Reinforced Cementitious Composites," *ASCE J. of Materials in Civil Engineering*, 4(1):41–57.
- Li, V. C., Y. Wang and S. Backer. 1990. "Effect of Inclining Angle, Bundling, and Surface Treatment on Synthetic Fiber Pull-Out from a Cement Matrix," *Composites*, 21(2):132–140.
- Loland, K. E. 1980. "Continuous Damage Model for Load-Response Estimation of Concrete," *Cement and Concrete Research*, 10:395–402.

- Marshall, D. B. and B. N. Cox. 1987. "Tensile Fracture of Brittle Matrix Composites: Influence of Fiber Strength," *Acta Metall.*, 35(11):2607-2619.
- Marshall, D. B., B. N. Cox and A. G. Evans. 1985. "The Mechanics of Matrix Cracking in Brittle-Matrix Fiber Composites," *Acta Metall.*, 33(11):2013-2021.
- Mihashi, H. 1983. "A Stochastic Theory for Fracture of Concrete," in *Fracture Mechanics of Concrete*, F. H. Wittmann, ed., Amsterdam: Elsevier Science, pp. 301-339.
- Prewo, K. M. and J. J. Brennan. 1982. "Silicon Carbide Yarn Reinforced Glass Matrix Composites," *J. Mater. Sci.*, 17:1201-1206.
- Shah, S. P. 1991a. "Toughening of Cement-Based Materials with Fiber Reinforcement," *Mat. Res. Soc. Sym. Proc.*, 211:3-13.
- Shah, S. P. 1991b. "Do Fibers Improve the Tensile Strength of Concrete?" in *Proc. First Canadian University-Industry Workshop on Fiber Reinforced Concrete*, N. Banthia, ed., Quebec: University of Laval, pp. 10-30.
- Spearing, S. M. and F. W. Zok. 1992. "Stochastic Aspects of Matrix Cracking in Brittle Matrix Composites," Report No. MS24, Materials Department, University of California, Santa Barbara.
- Sumarac, D. and D. Krajcinovic. 1989. "A Mesomechanical Model for Brittle Deformation Processes: Part II," *J. Applied Mechanics*, 56:57-62.
- Sutcu, M. 1989. "Weibull Statistics Applied to Fiber Failure in Ceramic Composites and Work of Fracture," *Acta Metall.*, 37(2):651-661.
- Weibull, W. 1951. "A Statistical Distribution Function of Wide Applicability," *J. Appl. Mech.*, 18:293.
- Wu, H. C. and V. C. Li. 1994. "Trade-off between Strength and Ductility of Random Discontinuous Fiber Reinforced Cementitious Composites," *J. Cement and Concrete Composites*, in press.
- Wu, H. C. and V. C. Li. 1992. "Snubbing and Bundling Effects on Multiple Crack Spacing of Discontinuous Random Fiber Reinforced Brittle Matrix Composites," *J. Am. Ceram. Soc.*, 75(12):3487-3489.
- Wu, H. C., T. Matsumoto and V. C. Li. 1994. "Buckling of Bridging Fibers in Composites," accepted for publication in *J. Mater. Sci. Lett.*
- Yang, X. F. and K. M. Knowles. 1993. "On the First-Matrix-Cracking Stress in Unidirectional Fiber-Reinforced Brittle Materials," *J. Mater. Res.*, 8(2):371-376.
- Yang, X. F. and K. M. Knowles. 1992. "The One-Dimensional Car Parking Problem and its Application to the Distribution of Spacings between Matrix Cracks in Unidirectional Fiber-Reinforced Brittle Materials," *J. Am. Ceram. Soc.*, 75(1):141-147.
- Zok, F. W. and S. M. Spearing. 1992. "Matrix Crack Spacing in Brittle Matrix Composites," *Acta Metall.*, 40(8):2033-2043.